

# Hard X-ray detection of NGC 1068 with BeppoSAX

G. Matt<sup>1</sup>, M. Guainazzi<sup>2</sup>, F. Frontera<sup>3</sup>, L. Bassani<sup>3</sup>, W.N. Brandt<sup>4</sup>, A.C. Fabian<sup>5</sup>, F. Fiore<sup>2,6</sup>, F. Haardt<sup>7</sup>, K. Iwasawa<sup>5</sup>, R. Maiolino<sup>8</sup>, G. Malaguti<sup>3</sup>, A. Marconi<sup>9,10</sup>, A. Matteuzzi<sup>2</sup>, S. Molendi<sup>11</sup>, G.C. Perola<sup>1</sup>, S. Piraino<sup>12</sup>, and L. Piro<sup>13</sup>

<sup>1</sup> Dipartimento di Fisica “E. Amaldi”, Università degli Studi “Roma Tre”, Via della Vasca Navale 84, I-00146 Roma, Italy

<sup>2</sup> SAX/SDC Nuova Telespazio, Via Corcolle 19, I-00131 Roma, Italy

<sup>3</sup> Istituto Tecnologie e Studio Radiazioni Extraterrestri, CNR, Via Gobetti 101, I-40129 Bologna, Italy

<sup>4</sup> Harvard-Smithsonian Center for Astrophysics, 60 Garden St., Cambridge, MA 02138, USA

<sup>5</sup> Institute of Astronomy, University of Cambridge, Madingley Road, Cambridge CB3 0HA, U.K.

<sup>6</sup> Osservatorio Astronomico di Roma, Via dell’Osservatorio, I-00044 Monteporzio-Catone, Italy

<sup>7</sup> Dipartimento di Fisica, Università di Milano, Via Celoria 16, I-20133 Milano, Italy

<sup>8</sup> MPI für Extraterrestrische Physik, Giessenbachstrasse 1, D-85748 Garching bei München, Germany

<sup>9</sup> Space Telescope Science Institute, 3700 San Martin Drive, Baltimore, MD 21218, U.S.A.

<sup>10</sup> Dipartimento di Astronomia e Scienza dello Spazio, Largo E. Fermi 5, I-50125 Firenze, Italy

<sup>11</sup> Istituto di Fisica Cosmica e Tecnologie Relative, Via Bassini 15, I-20133 Milano, Italy

<sup>12</sup> Istituto di Fisica Cosmica ed Applicazioni dell’Informatica, Via Ugo La Malfa 153, I-90146 Palermo, Italy

<sup>13</sup> Istituto di Astrofisica Spaziale – C.N.R., Via E. Fermi 21, I-00044 Frascati, Italy

Received / Accepted

**Abstract.** We report on the first detection above  $\sim 10$  keV of the archetypal Compton-thick Seyfert 2 galaxy NGC 1068. This detection, obtained with the PDS instrument onboard BeppoSAX in the 20–100 keV range, confirms the hardness of the X-ray spectrum above a few keV (as indicated by ASCA observations) and supports models envisaging a mixture of both neutral and ionized reflections of an otherwise invisible nuclear continuum, the neutral reflection component being the dominant one in hard X-rays.

**Key words:** X-rays: galaxies – Galaxies: Seyfert – Galaxies: individual: NGC1068

## 1. Introduction

NGC 1068 is the archetypal object for both the class of Seyfert 2 galaxies as a whole and the Compton-thick subclass (see Matt 1997 for a brief review), i.e. those objects for which the column density of the line-of-sight absorbing matter (hereinafter identified with the torus, see e.g. Ward 1996) exceeds  $\sigma_T^{-1} = 1.5 \times 10^{24}$  cm<sup>-2</sup> and is therefore optically thick to Compton scattering. A column of a few times this critical density is sufficient to strongly depress the transmitted intensity also in hard X-rays, since after a few scatterings photons are redshifted into the photoelectric dominated regime. However, even for very high column densities, nuclear radiation can still

be observed in scattered light, as both the visible part of the inner surface of the torus and the warm medium responsible for scattering and polarizing the optical broad lines (Antonucci & Miller 1985) can act as mirrors (e.g. Ghisellini et al. 1994; Matt et al. 1996). The two reflectors produce rather different spectra: the torus is supposed to be essentially neutral, then giving rise to the so-called Compton reflection continuum (Lightman & White 1988); the warm mirror should be highly ionized, and its spectral shape basically the same as the nuclear one, apart from a high energy cutoff owing to Compton downscattering. Superimposed on both continua, emission lines are also expected, iron lines being the most prominent: a 6.4 keV fluorescent line from the torus, highly ionized resonant scattering and fluorescence/recombination lines from the warm mirror (such as reported by Matt et al. 1996).

This two-reflectors picture is confirmed (and it has been partly motivated) by ASCA observations of NGC 1068 (Ueno et al. 1994; Iwasawa et al. 1997), which clearly distinguished three different iron lines: one at 6.4 keV, the other two consistent with He- and H-like iron, respectively (the lines being possibly redshifted by a few thousands km/s, Iwasawa et al. 1997) with equivalent widths of the order of 1 keV each, as expected in the reflection model (Matt et al. 1996). The continuum is not well constrained by ASCA due to the limited energy range available for its evaluation (below 4 keV a thermal-like component dominates, Ueno et al. 1994), but it looks very flat, as expected if the cold reflector were providing a significant contribution.

To confirm this scenario, hard X-rays observations are necessary. We then proposed to observe NGC 1068 with BeppoSAX, in order to take full advantage of the good sensitivity

Send offprint requests to: G. Matt (matt@amaldi.fis.uniroma3.it)

of the PDS, the Phoswich Detector System working between 15 and 300 keV. In fact, a cold reflection-dominated spectrum would be hard enough to be observable with the PDS with a  $\sim 10^5$  s pointing even at the relatively low flux level of NGC 1068 (i.e. about a quarter of a mCrab<sup>1</sup> between 2 and 10 keV). Here we report what is to our knowledge the first detection of NGC 1068 up to 100 keV.

## 2. Data reduction

The X-ray satellite BeppoSAX (Boella et al. 1997a), a program of the Italian space agency (ASI) with participation of the Netherlands agency for Aerospace Program (NIVR), includes four co-aligned Narrow Field Instruments: a Low Energy Concentrator Spectrometer (LECS), three Medium Energy Concentrator Spectrometers (MECS), a High Pressure Gas Scintillation Proportional Counter (HPGSPC), and a Phoswich Detector System (PDS). The LECS and MECS have imaging capabilities and cover the 0.1–10 keV and 1.3–10 keV energy ranges respectively; in the overlapping band the total effective area of the MECS (which is  $\sim 150$  cm<sup>2</sup> at 6 keV) is about three times that of the LECS. The energy resolution is  $\sim 8\%$  and the angular resolution is  $\sim 1.2$  arcmin (Half Power radius) at 6 keV for both instruments. The HPGSPC and the PDS are collimated instruments covering the 4–120 keV and the 15–300 keV energy ranges respectively. In the overlapping band the PDS is more sensitive, the best characteristic of the HPGSPC being instead the good energy resolution.

BeppoSAX observed the source from December 30 1996 to January 3 1997 for about 110 ks effective time. In this paper we present only MECS (Boella et al. 1997b) and PDS (Frontera et al. 1997) data, because of our choice to restrict the analysis to energies greater than 4 keV (see next section).

MECS spectra have been extracted from a 4 arcmin radius region around the centroid of the source image; the spectra from the three units have been equalized to the MECS1 energy–PI relationship and added together. Since the MECS background is very low and stable<sup>2</sup>, data selection is straightforward; we used all data acquired with an angle, with respect to the Earth limb, higher than  $5^\circ$ . The background subtraction has been performed using blank sky spectra extracted from the same region of the detector field of view.

The PDS consists of four units, and was operated in collimator rocking mode, with a pair of units pointings to the source and the other pair pointings  $\pm 210$  arcmin away, the two pairs switching on and off source every 96 seconds. The net source spectra have been obtained by subtracting the ‘off’ to the ‘on’ counts. Then the spectra of the four crystals have been summed together after performing gain equalization. A slight improvement in the S/N has been obtained by optimizing the Rise Time selection: only events in the range 5–133 (digital units; see Fig.

2 of Frontera et al. 1997) have been used. This choice guarantees no reduction in the detection efficiency due to pulse shape analysis. Isolated spikes, likely due to short particle “bursts”, have been removed. Data within 5 minutes after any South Atlantic Anomaly passage have been discarded to avoid gain problems due to high voltage recovery after instrument switch-off. The total effective on-source time is  $T_{\text{exp}}=65000$  s. The net count rate (CR) is  $0.15 \pm 0.03$  cts/s, corresponding to a 20–200 keV flux  $\sim 1.3$  mCrab if a simple power-law with  $\Gamma=2$  is assumed (note that this flux is well below the OSSE and SIGMA upper limits, McNaron–Brown et al., in preparation, Jourdain et al. 1994).

As a further check, we have divided the whole observation in three temporal segments; the net count rates are all consistent one another:  $CR_{\text{first}} = 0.15 \pm 0.05$  cts/s ( $T_{\text{exp}} \simeq 22400$  s),  $CR_{\text{second}} = 0.13 \pm 0.05$  cts/s ( $T_{\text{exp}} \simeq 20300$  s),  $CR_{\text{third}} = 0.15 \pm 0.05$  cts/s ( $T_{\text{exp}} \simeq 21800$  s).

Deep observations of blank fields show that the systematic residuals in the background subtraction procedure are at most 0.25 mCrab in the 20–200 keV energy range where the PDS response matrix is currently well calibrated. Even if this maximum value were subtracted from the observed count rate, the S/N would remain  $> 4\sigma$ .

We have also checked for the presence of contaminating sources in the  $\simeq 1.3^\circ$  PDS field of view. No source at a flux level  $> 0.03$  mCrab in the 2–10 keV band is reported in X-ray catalogs. In particular, no source is present neither in the PDS field of view nor in an annulus at angle  $\theta \simeq 210$  arcmin from the pointing position in the hard X-ray extragalactic sources catalog of Malizia & Bassani (1996).

## 3. Spectral analysis and results

Spectral fits have been performed with the XSPEC 9.0 package, using the response matrices released on Jan 1997. To cure the mismatch between MECS and PDS absolute normalizations in the current matrices, PDS data have been divided by a factor 0.7, constant over energy (Cusumano et al., in preparation). Note that even allowing for a 10% remaining uncertainty in the cross-calibration, the continuum best fit parameters would change only slightly, and the basic picture would by no means be altered.

In the following, all quoted errors correspond to 90% confidence level for one interesting parameter ( $\Delta\chi^2=2.7$ ).

As we are interested here only in the high energy part of the spectrum (i.e. that believed to be due to the reflection of the obscured nucleus), we restricted our analysis to energies greater than 4 keV to avoid contamination from other spectral components. The overall spectrum between 4 and 100 keV is shown in Fig.1. The spectrum confirms that NGC 1068 is substantially Compton-thick, otherwise it would have been detected at a much higher level in hard X-rays, similarly to NGC 4945 (Iwasawa et al. 1993; Done et al. 1996). A prominent, broad iron line is clearly seen. According to ASCA–SIS results (Ueno et al. 1994; Iwasawa et al. 1997), we fitted this broad feature with a blend of three narrow lines, with energies fixed at 6.4

<sup>1</sup> 1 mCrab= $2.4 \times 10^{-11}$  and  $3 \times 10^{-11}$  erg cm<sup>-2</sup> s<sup>-1</sup> in the 2–10 and 20–200 keV ranges, respectively.

<sup>2</sup> For information on the background and on data analysis in general see <http://www.sdc.asi.it/software/cookbook>

keV (corresponding to neutral iron), 6.7 keV (He-like iron) and 6.97 keV (H-like iron), respectively. The results are presented in Table 1, and have been obtained adopting a power law for the continuum (fitted to MECS data only). No significant differences in the parameters of the lines have been found with a more complex description of the continuum (see below). If the ionized lines energies are instead fixed at 6.61 and 6.86 keV, as suggested by Iwasawa et al. (1997), the results are somewhat different, the H-like line being now more intense than the He-like one. Leaving these energies free, the best fit values are 6.64 and 7.01 respectively (but consistent within the errors with the nominal atomic values). From a statistical point of view, the first and third fits seem to be preferred, but all three results are acceptable at the 90% confidence level. The power law index of the underlying continuum is insensitive to the details of the line modeling. What is important to remark is that the lines' equivalent widths are of the expected order if these lines were produced by reflection of an invisible primary radiation (Matt et al. 1996).

If the MECS+PDS continuum is fitted with a simple power law, a good fit is obtained (see Table 2). (The iron lines have been modeled for simplicity with a single, broad gaussian feature). However, fitting the PDS data alone gives a photon index of  $1.83_{-0.52}^{+0.72}$ , inconsistent at the 90% level with the index of the total spectrum. This is due to the fact that the index is driven basically by the MECS, owing to its better statistics, while the PDS data, even if lying, on average, on the extrapolation of the lower energy spectrum, have a different spectral shape. This high energy steepening, together with the flatness of the 4–10 keV continuum and the presence of a strong 6.4 keV iron line suggests that part of the continuum is due to reflection of the nuclear radiation by circumnuclear neutral matter, possibly the inner surface of the torus. The presence of intense He- and H-like iron lines, and the fact that the 4–10 keV continuum, even if flatter than usual in Seyfert galaxies, is not as flat as a pure cold reflection spectrum would be, indicates contribution from an ionized reflector too, to be identified with the same medium responsible for the scattering and polarization of the optical broad lines. We then fitted the MECS+PDS continuum with a cold reflection component (XSPEC's model PLREFL) plus reflection from free electrons, i.e. a power law with Compton downscattering in the assumption of a parallel incident beam and temperature of the electrons negligible with respect to the photon energy; in formulae (e.g. Matt 1996 and Poutanen et al. 1996):

$$I(E) = \frac{3\sigma_T}{16\pi} \left( \frac{d\Omega}{4\pi} \right) \left[ \frac{E}{E_0} + \frac{E_0}{E} - \sin^2 \theta \right] I(E_0) , \quad (1)$$

where  $\theta$  is the scattering angle,  $d\Omega$  the solid angle subtended by the illuminated matter, and

$$E_0 = \frac{E}{1 - (E/mc^2)(1 - \cos \theta)} . \quad (2)$$

The power law index of the illuminating radiation has been assumed to be the same for the two reflection components (so

assuming no angular dependence of the nuclear emission spectral shape). To agree with the current wisdom on Seyfert 1 X-ray spectra, a reflection component from the accretion disc should actually have been included in modeling the nuclear radiation; however, it appears to be an unnecessary sophistication here. The fit results are shown in Table 2, and the best fit model in Fig. 2. The power law index of the primary emission ( $1.74_{-0.56}^{+0.25}$ ) is consistent with typical Seyfert 1 values (Nandra & Pounds 1994). The scattering angle  $\theta$  (which, with our assumptions, is the same as the system inclination angle) is unfortunately not constrained, affecting the spectrum only at the highest energies, where the statistics is poor. The warm reflection component is the most important in the 4–10 keV range, while the cold reflection component dominates above 10 keV (see Fig. 2).

If the nuclear X-ray luminosity is of the order of  $10^{44}$  erg  $s^{-1}$ , as indicated by several and independent pieces of evidence (Iwasawa et al. 1997 and references therein), then the 20–100 keV observed flux is about 2 orders of magnitude lower than the nuclear one. Adopting the Ghisellini et al. (1994) geometry, both a very high equatorial column density of the torus ( $\gtrsim 10^{26}$   $cm^{-2}$ ) (to avoid a significant transmitted intensity) and a high inclination angle (to reduce the observable fraction of the inner surface of the torus) are implied (see Fig. 6 of Ghisellini et al. 1994). A high inclination disagrees with estimates based on both polarization properties (Miller et al. 1991), assuming that the X-ray and optical/near IR scatterers are one and the same, and infrared mapping of the torus (Young et al. 1996); such a disagreement would suggest that either the geometry is more complex than commonly assumed or the luminosity is smaller than estimated. Interestingly, however, both the large column density and the high inclination are consistent with recent water maser measurements (Gallimore et al. 1996; Greenhill et al. 1996).

#### 4. Summary

We have reported on the detection of the Seyfert 2 galaxy NGC 1068 up to 100 keV, obtained with the PDS instrument onboard BeppoSAX. This is the first time that a Compton-thick Seyfert 2 is detected at so high energies, supporting the scenario in which medium to hard X-rays are due to reflection, from both ionized and neutral circumnuclear media, of an otherwise invisible nuclear radiation.

*Acknowledgements.* We thank all the people who, at all levels, have made possible the SAX mission. This research has made use of SAX-DAS linearized and cleaned event files (rev0.1) produced at the BeppoSAX Science Data Center. GM and GCP acknowledge financial support from an ASI grant, AMar from STScI (GO grant G005.44800).

#### References

- Antonucci R.R.J., Miller J.S., 1985, ApJ, 297, 621
- Boella G., Butler R.C., Perola G.C., et al., 1997a, A&AS, 112, 299
- Boella G., Chiappetti L., Conti G., et al., 1997b, A&AS, 112, 327
- Done C., Madejski G.M., Smith D.A., 1996, ApJ, 463, L63
- Frontera F., Costa E., Dal Fiume D., et al., 1997, A&AS, 112, 357

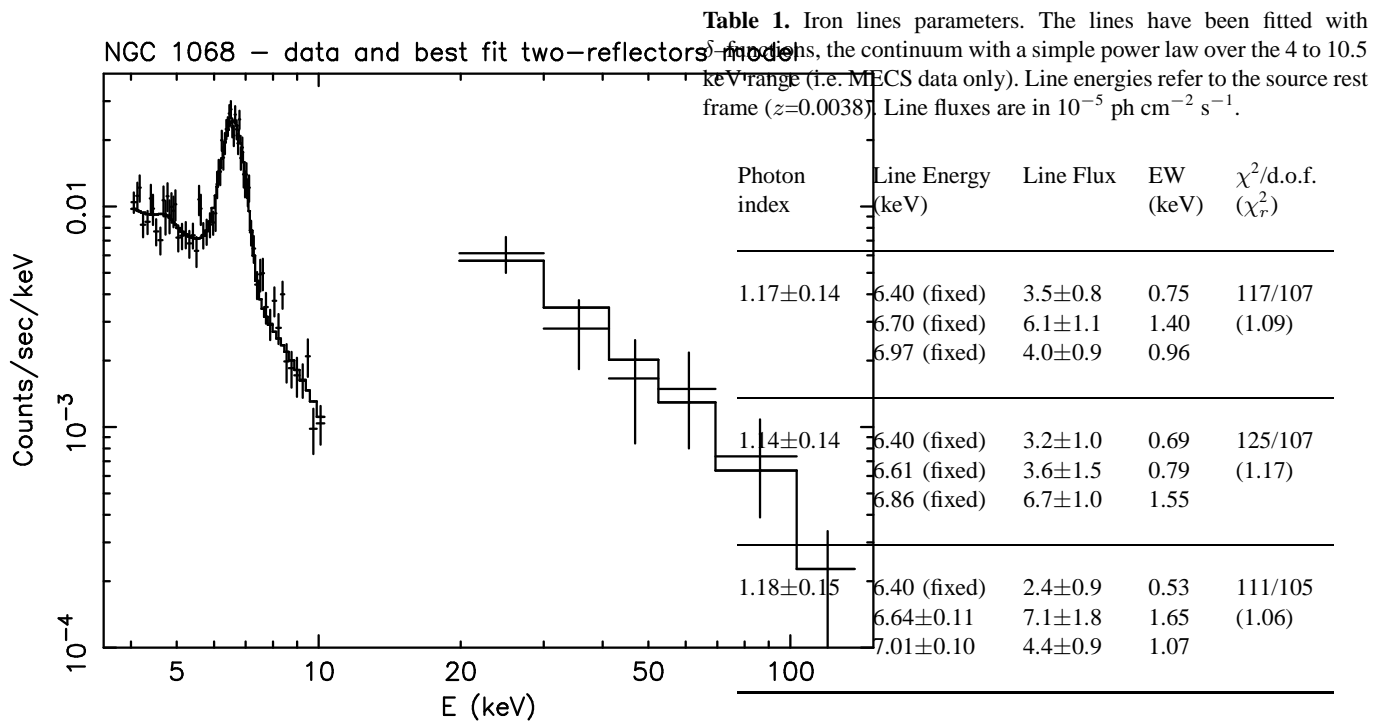


**Fig. 1.** The observed BeppoSAX spectrum of NGC 1068 (folded with the instruments response) above 4 keV. Best fit parameters (two-reflectors model) are given in Table 2.

**Table 2.** MECS+PDS joint fits with either a simple power law or the two-reflectors model (see text for details). Fluxes are in  $10^{-12}$  erg cm $^{-2}$  s $^{-1}$  and refer to the continuum only. C and W stand for the cold and warm reflector respectively.

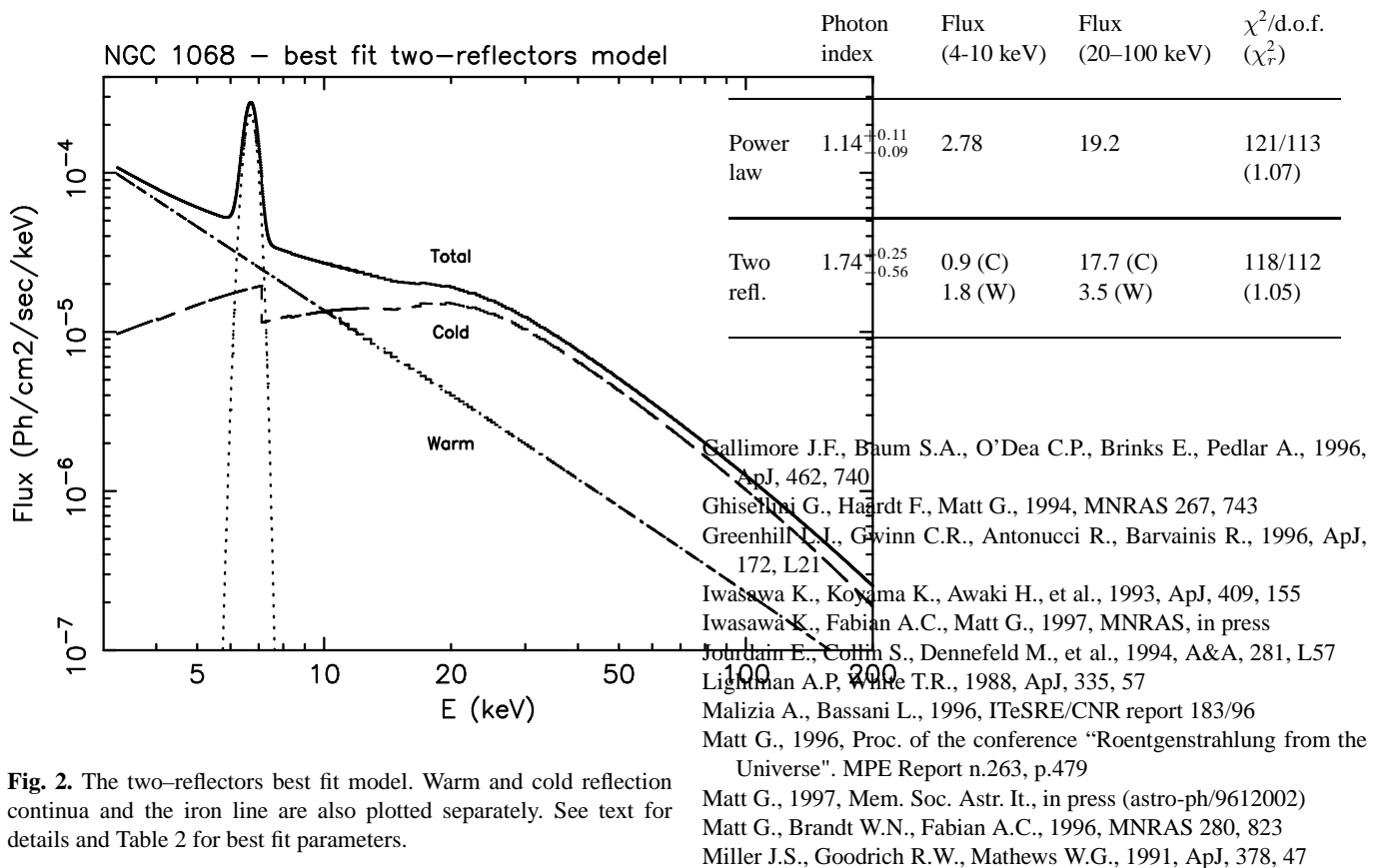


**Fig. 2.** The two-reflectors best fit model. Warm and cold reflection continua and the iron line are also plotted separately. See text for details and Table 2 for best fit parameters.

- Nandra K., Pounds K.A., 1994, MNRAS 268, 405  
Poutanen J., Sikora M., Begelman M.C., Magdziarz P.: 1996, ApJ 465,  
L107  
Ueno S., Mushotzky R.F., Koyama K., et al., 1994, PASJ 46, L71  
Ward M.J, ed., 1996, Proceedings of the Workshop "Evidence for the  
Torus", Vistas in Astronomy, 40  
Young S., Packham C., Hough J.H., Efstathiou A., 1996, MNRAS,  
283, L1